

# Learning Wake Regimes from Snapshot Data

Maziar S. Hemati\*

*University of Minnesota, Minneapolis, MN 55455, USA*

Fluid wakes are often categorized by visual inspection according to the number and grouping of vortices shed per cycle (e.g., 2S, 2P, P+S). While such categorizations have proven useful for describing and comparing wakes, the criterion excludes features that are essential to a wake’s evolution (i.e., the relative positions and strengths of the shed vortices). For example, not all 2P wakes exhibit the same dynamics; thus, the evolution of wake patterns among 2P wakes can be markedly distinct. Here, we explore the notion of labeling wakes according to their dynamics based on empirical snapshot data. Snapshots of the velocity field are reduced to a representative feature vector, which is then processed using machine learning techniques tailored to the task of wake regime learning. The wake regime learning framework is evaluated on an idealized 2P wake model, which can be configured to simulate different (known) dynamical regimes. A simple version of the wake regime learning framework successfully discriminates between dynamically distinct 2P wakes. The results presented here suggest that the wake regime learning perspective may facilitate the development of a new dynamics-based wake labeling convention in the future.

## I. Introduction

Biological swimmers exhibit a remarkable ability to exploit complex fluid-structure interactions to maneuver and propel themselves through their fluid environments. A better understanding of their ability to do so has great potential to inform the design of robotic locomotors and human-engineered systems. To this end, many investigators have studied the wide spectrum of gaits and undulatory kinematics exhibited by marine swimmers.<sup>1,2</sup> Of course, the body kinematics only tell one side of the story, since locomotion in a fluid medium is intimately coupled with the fluid dynamics as well. As such, innumerable other studies have considered *both* the nature of the body kinematics as well as the nature of the fluid wakes generated from these gaits.<sup>3–12</sup> For instance, it has been observed that “mackerel-like” carangiform swimmers typically generate “2S” wake patterns (i.e., two *single* vortices are shed per oscillation cycle), whereas “eel-like” anguilliform swimmers mainly generate “2P” (i.e., two *pairs* of vortices shed per oscillation cycle) and more complex “higher-order” wake patterns.<sup>10</sup>

The attention given to wake patterns and the associated wake formation process has facilitated the study of fluid-structure interactions arising in swimming locomotion and other contexts. In fact, wake patterns have been the focus of many studies in fluid dynamics,<sup>13–17</sup> which ultimately led to a wake labeling scheme for describing wakes across application areas—according to the number and grouping of vortices shed per cycle (e.g., “2S” and “2P”). Wake labels of this type were first utilized by Williamson and Roshko, as a means of objectively studying the dependence of wake patterns across the parameter space associated with an oscillating cylinder in a uniform flow.<sup>18</sup> The ability to objectively compare wake patterns as either similar or dissimilar, using Williamson and Roshko’s labeling scheme—herein referred to as the *WR labeling scheme*—has had a tremendous impact on the manner in which wake flows are viewed and studied—so much so that the WR labeling scheme has been invoked to label exotic wake patterns beyond those originally observed by Williamson and Roshko (e.g., “3P+S”<sup>19</sup> and “6P+2S”<sup>20</sup>). In the context of swimming locomotion, the WR wake labeling criterion has been used to describe the 2S and 2P wakes that arise at various “wake resonance” modes.<sup>21,22</sup> Further, both the 2S wake pattern—in the form of a reverse von Kármán street—and the 2P wake pattern have been associated with thrust generation in biological swimmers.<sup>9</sup> Owing to observations such as these, 2S and 2P wake patterns are often targeted in bio-inspired robot design and used to evaluate the performance of swimming robots.<sup>23,24</sup>

---

\*Assistant Professor, Department of Aerospace Engineering and Mechanics. Member AIAA, mhemati@umn.edu.

Despite the utility of the WR labeling scheme in comparing wake patterns in an objective manner across application areas, the criterion involved in ascribing labels to these wake patterns does not provide a *complete* description of a wake. For instance, not all 2P wakes are equivalent from the standpoint of their dynamics; while two different wakes may be labeled as 2P, the evolution of these patterns can be markedly different. Indeed, the evolution of a wake pattern is dictated by more than the number and grouping of vortices shed per cycle, but also by the relative positions and strengths of these vortices: a well established fact in the vortex dynamics literature.<sup>25–30</sup> This fact indicates that the number and grouping of vortices alone (i.e., labels as 2S, 2P, P+S, and the like) may be insufficient to distinguish between wake regimes; such categorizations can potentially fail to pick out sub-classifications that can be made from the perspective of the wake *dynamics*. For instance, in the recent study by Basu and Stremler, an idealized point vortex model of a 2P wake was thoroughly examined and found to exhibit five distinct dynamical behaviors, manifested in the form of qualitatively different patterns in the vortex trajectories.<sup>30</sup> The five general classes of motion for the idealized 2P wake system—orbiting, exchanging, scattering, passing, and mixed—are further divided into dynamical sub-regimes, leading to a total of 12 distinct classes of motion.<sup>30</sup>

While the analysis performed on idealized point vortex models does not necessarily translate directly into physical reality, the existence of dynamically distinct wake regimes in such models does raise questions about the “resolution” provided by the WR wake classification scheme. For example, multiple wakes labeled as “2P” could possess significant dynamical differences that, depending on context, could be essential when comparing wakes; conclusions drawn from the WR labeling criterion can be significantly different from conclusions drawn from a comparison of the wake dynamics. Indications of the breakdown of the WR labeling scheme for certain comparisons has already become evident in the literature. For instance, Schnipper et al. observe *drag producing* 2P wakes in experiments of a flapping foil,<sup>20</sup> whereas the 2P wakes they aimed to study were motivated by the *thrust generating* 2P wakes observed in undulatory swimming.<sup>9</sup> As a matter of fact, Schnipper et al. identify and describe specific differences between the trailing edge vortex formation process between their experimental foils and fish swimmers, suggesting that the wake patterns could be distinguished as dynamically different. Observations like these highlight a need for expanding the current lexicon to include a naming convention that enables wakes to be compared and contrasted according to their dynamics. It seems that by appealing to the *evolution* of the wake patterns, a more refined categorization of wakes can be established—one that labels wakes according to dynamical regimes. A finer labeling criterion may lead to new insights about wakes, providing a framework through which to compare and analyze wakes according to the (dis)similarity of their dynamics. Such a scheme would provide for greater resolution in the study of wakes, which could potentially be used to reconcile discrepancies in wake characteristics observed as a result of comparing wakes according to the number and grouping of vortices alone.

In principle, a richer dynamics-based labeling scheme could be developed by considering the patterns exhibited in the vortex trajectories, as determined from empirical snapshot sequences of, e.g., the velocity field. Such a method would be akin to the convention used by Basu and Stremler for *naming* various dynamical regimes associated with an idealized 2P wake.<sup>30</sup> Here, we note that the vortex trajectories alone are not the only metric that can be used for delineating between various regimes of motion. Patterns observed in the vortex trajectories are but one choice of “feature” that can be used for this task. Here, rather than focus on a labeling convention based solely on vortex trajectories, we consider a general framework for wake regime learning based on dynamically relevant features extracted from available sets of snapshot data. In particular, we explore the possibility of applying dimension reduction and machine learning techniques directly on empirical snapshot sequences of the velocity field—gathered from a variety of parameter regimes—as a means of clustering velocity fields according to similarities in the underlying dynamics. Such an approach would then provide a general foundation upon which to build *flow regime learning* techniques for a broader class of fluid flows, beyond vortex wakes and vortex-dominated flows.

We note that while a number of other studies have been conducted on the application of machine learning techniques for the analysis of fluid flows and wakes, none have focused on the specific problem of *wake regime learning* that is considered here. For example, fuzzy clustering techniques have been employed in the study of wakes—in conjunction with the proper orthogonal decomposition (POD)—as a means of determining “dominant structures” underlying the flow;<sup>31</sup> much of the work focused on the question of identifying dominant POD modes and their contributions to the resulting 2S or 2P wake structures observed in experiments. A series of machine learning techniques have also been applied to estimate the parameters of a flow from various datasets. Nonlinear manifold learning techniques, such as the isometric feature mapping (Isomap) method, have been shown to be useful in estimating Reynolds number from raw video footage

of cylinder wakes.<sup>32</sup> Similar success has been demonstrated through a combined use of POD, compressive sensing, and supervised learning to determine the Reynolds number associated with numerically simulated cylinder flows from a limited set of surface pressure signals.<sup>33,34</sup> Related techniques have been successful in the context of separated flows for discriminating between actuated and unactuated flows from image data.<sup>35</sup> These latter techniques can potentially be leveraged for wake regime *classification*—a supervised learning problem aimed at labeling a single snapshot realization of a wake according to an already established library of features and labels; of course, such a notion is predicated on the availability of a suitable library of wake regime labels and features. One outcome of the (unsupervised) wake regime learning approach considered here is an ability to construct such a library for these classification tasks, purely from empirical snapshot data.

In this work, our goal is to partition a collection of experimental or numerical datasets of fluid wakes (e.g., snapshot sequences of the velocity field) into cohesive clusters according to similarities in the associated wake dynamics. To this end, we present a general framework for wake regime learning and explore the possibility of using a data-driven framework—combining ideas from dimension reduction, low-rank approximation, data-driven dynamical systems, and machine learning—to address this challenge. Since this work is exploratory, we focus on the wake regime learning problem in a proof-of-concept manner. We utilize idealized wake models, for which dynamical sub-classifications are already known, to serve as a rich model problem for verification and validation of our wake regime learning algorithms. In particular, we conduct our studies in the context of idealized 2P wakes, owing to the prevalence of 2P wakes in swimming locomotion and vortex induced vibrations.<sup>16</sup> Snapshots of the velocity field from numerous “unlabeled” regimes are processed and categorized according to similarities in dynamically relevant features extracted from each snapshot sequence. We find that even very simple techniques can be used to correctly label snapshot data according to the dynamical regimes underlying idealized vortex wake models; however, further investigation is needed to refine the performance of the techniques.

In Section II, we propose a general framework for wake regime learning that consists of a feature extraction stage and a clustering stage. In order to evaluate and assess the performance capabilities of the wake regime learning algorithms, we present an idealized point vortex wake model in Section III. The vortex model is used to explicitly show that the WR labeling scheme omits information essential to describing the wake dynamics; further, these idealized wake models provide a rich and convenient environment for studying the wake regime learning problem in greater detail. The capabilities of a specific implementation of the wake regime learning framework are studied in the context of an idealized 2P wake model in Section IV. Discussion and concluding remarks are presented in Section V.

## II. A General Framework for Learning Wake Regimes from Snapshot Data

Consider the snapshot data sequence  $X = [x_1 \ x_2 \ \dots \ x_m] \in \mathbb{R}^{n \times m}$  that has been generated empirically, either in numerical simulation or in experiment. Here,  $m$  is the number of snapshots in the sequence and  $n$  is the dimension of each snapshot. Wake regime learning aims to partition a set of  $R$  empirical realizations of wake snapshot sequences  $\mathcal{X} = \{X^{(1)}, \dots, X^{(R)}\}$  into  $K$  cohesive clusters sorted by dynamical regime; that is, each wake realization  $X^{(r)}$  should be grouped into a set of clusters  $C \in \{C_1, \dots, C_K\}$ , where each  $C_k$  is a set of wake realizations with similar dynamics. For wake regime learning, the individual snapshots are usually associated with the velocity or vorticity field, though other quantities can also be considered.

In general terms, the wake regime learning problem is one of *temporal clustering*. A cluster is a set of similar objects, with similarity defined in terms of some distance measure. For wake regime learning, the distance measure must be able to partition wake snapshot data into clusters with similar dynamics. Here, we propose to transform the temporal clustering problem into a non-temporal clustering problem by representing each realization of wake snapshot data as a corresponding *feature vector*  $\phi$ . For example, many temporal clustering methods make use of the time-series statistics (e.g., mean, skew, and kurtosis) as representative features. In the wake regime learning problem, the choice of feature vectors must be able to effectively discriminate between similar/dissimilar wake dynamics. While determining the most suitable features for this task presents a challenge, the proper choice of a suitable feature vector allows for the temporal clustering problem to be transformed into a non-temporal clustering problem. The general wake regime learning framework considered here consists two stages, depicted graphically in Figure 1:

1. *Feature extraction.* For each wake realization  $X^{(r)}$ , extract a feature vector  $\phi^{(r)}$ ;

2. *Clustering.* Perform unsupervised learning on the set of feature vectors from all  $R$  wake realizations  $\Phi = \{\phi^{(1)}, \dots, \phi^{(R)}\}$  to partition the collection of snapshot sequences into  $K$  clusters  $\{C_1, \dots, C_K\}$ .

While the spirit of the two stage approach presented here is relatively straightforward, the details of each of these two stages need to be studied further. For example, the best set of features—if one exists for the wake data at hand—is unknown and must be determined for effective wake regime learning. Further, practical considerations such as noise, outliers, and missing data can influence the reliability of a particular approach, even when the techniques show promise in an ideal setting. In the following section, we describe the particular choice of feature vector and clustering algorithm considered in the present study. These choices are made as much based on simplicity and convenience as they are based on relevance to the wake learning task. A closer study of features and clustering approaches is the focus of ongoing work.

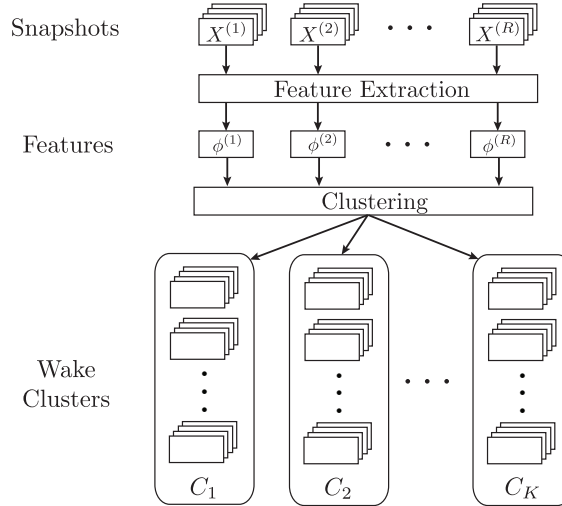


**Figure 1:** The wake regime learning framework presented here aims to sort a set of  $R$  wake snapshot sequences  $\mathcal{X} = \{X^{(1)}, X^{(2)}, \dots, X^{(R)}\}$  into  $K$  groups with similar dynamics through a general two-stage procedure consisting of feature extraction and clustering.

## A. Feature Extraction and Clustering

Suitable features for the wake learning task must be able to partition the snapshot data according to the wake dynamics. Further, these features must be determined such that they encapsulate spatiotemporal information in a *concise* manner. While numerous options exist, in the context of the present study, we utilize feature vectors based on the singular value decomposition (SVD) of the snapshot sequence  $X^{(r)} = U\Sigma V^*$ . In particular, we define the feature vector as the absolute value of the dominant left-singular-vector  $u$ ,

$$\phi^{(r)} = |u|. \quad (1)$$

This choice is motivated by problems in low-rank approximation,<sup>36</sup> and is equivalent to a feature vector determined as the absolute value of the dominant POD mode for a given snapshot sequence (without mean subtraction). In consideration of the physical insights gleaned from the idealized wake models to be discussed in Section III, these spatial modes are expected to reflect the essential features of the vortex evolution, without reverting to an explicit vortex identification and tracking procedure. Lastly, we note that feature vectors based on a larger number of POD modes scaled by associated spectral energy were also considered, but with little added value. Alternatives to POD-based features were also considered, including Fourier modes/frequencies and dynamic mode decomposition (DMD) modes/eigenvalues;<sup>37,38</sup> however, these alternative choices of features either deteriorated the accuracy of the clustering, or led to little notable differences in performance. Further exploration of alternative feature vectors is ongoing; only the results corresponding to features determined by (1) are reported here. Ultimately, a feature vector that provides the “best” distinction between dynamical regimes in the most concise and reliable fashion will be the best choice from

a practical standpoint; however, the performance of the wake learning framework will also be coupled with the particular clustering approach selected in the implementation.

As in the feature extraction stage, many options are available for clustering and unsupervised learning. In this study, we make use of the popular  $k$ -means clustering technique.<sup>39,40</sup> The  $k$ -means clustering problem statement follows: given  $R$  feature vectors  $\{\phi^{(1)}, \phi^{(2)}, \dots, \phi^{(R)}\}$ , partition the data into  $K \leq R$  sets (clusters)  $C \in \{C_1, C_2, \dots, C_K\}$  such that the within-cluster sum of squares is minimized. That is,

$$\operatorname{argmin}_C \sum_{k=1}^K \sum_{\phi \in C_k} \|\phi - \mu_k\|^2, \quad (2)$$

where  $\mu_k$  denotes the centroid of feature vectors in cluster  $C_k$ . The  $k$ -means clustering algorithm solves this optimization problem iteratively; however, when the technique converges to a solution, that solution is only a local minimizer—not necessarily a global minimizer. To reconcile this problem, we make use of 100 independent invocations of the  $k$ -means algorithm, each based on a different random initial seed. Additionally, to improve robustness to outliers that can potentially arise near the boundaries between wake regimes, we implement the  $k$ -means algorithm based on an  $\ell_1$ -norm minimization criterion, rather than the sum of squares criterion that is typically applied.

We emphasize that the results in this study are based on feature vectors and clustering algorithms that were chosen for their simplicity and convenience. Future work will consider alternative and more sophisticated techniques for optimizing the performance of the approach in various contexts.

### III. Point Vortex Modeling of Exotic Wake Dynamics

Idealized point vortex representations of bluff body wakes—extensively studied in the vortex dynamics literature<sup>25,27</sup>—provide a convenient context for developing and validating wake regime learning techniques. These models are especially useful for algorithm testing and evaluation because the regimes of motion can be determined from the models directly, thus allowing for an objective validation of the data-driven techniques. Here, we summarize the basic formulation of idealized wake models and present the special case of an idealized 2P wake that will be used to demonstrate the data-driven wake regime learning framework in Section IV. Further details about these vortex wake models can be found in the recent works by Stremmer and colleagues.<sup>28–30</sup>

The vorticity  $\omega(z, t)$ , as a function of complex position  $z = x + iy$  and time  $t$ , can be represented by a system of  $N$  point vortices as

$$\omega(z, t) = \sum_{\alpha=1}^N \Gamma_{\alpha} \delta(z - z_{\alpha}(t)), \quad (3)$$

where  $\Gamma_{\alpha} \in \mathbb{R}$  and  $z_{\alpha}(t) \in \mathbb{C}$  denote the strength and complex position of vortex  $\alpha$ , respectively. Here, we assume that the vortex strengths remain constant in time. In the unbounded domain, a system of  $N$  point vortices evolves according to<sup>41,42</sup>

$$\frac{dz_{\alpha}^*}{dt} = \frac{1}{2\pi i} \sum_{\substack{\beta=1 \\ \beta \neq \alpha}}^N \frac{\Gamma_{\beta}}{z_{\alpha} - z_{\beta}}, \quad (4)$$

where  $(\cdot)^*$  denotes complex-conjugation.

In modeling the evolution of vorticity in a bluff-body wake, we instead consider the evolution of  $N$  vortices in a strip of a singly-periodic domain. Thus, we account for the mutual interactions between all the vortices in a given strip (as in (4)), as well as the interactions with all of the vortices in the strips along the periodic direction (taken as  $x$  here). Taking the length of a single strip to be  $L \in \mathbb{R}$ , the equations of motion for the  $N$  point vortices in the base strip  $x \in [0, L)$  can be expressed as

$$\frac{dz_{\alpha}^*}{dt} = \frac{1}{2\pi i} \sum_{\substack{\beta=1 \\ \beta \neq \alpha}}^N \sum_{\kappa=-\infty}^{+\infty} \frac{\Gamma_{\beta}}{z_{\alpha} - z_{\beta} + \kappa L}, \quad (5)$$

which, by periodicity, governs the evolution of all vorticity in the singly-periodic domain. This expression can be further simplified by noting the identity  $\pi \cot \pi x = \sum_{\kappa=-\infty}^{\infty} (x + \kappa)^{-1}$ , which yields the equivalent

expression

$$\frac{dz_\alpha^*}{dt} = \frac{1}{2Li} \sum_{\substack{\beta=1 \\ \beta \neq \alpha}}^N \Gamma_\beta \cot \left[ \frac{\pi}{L} (z_\alpha - z_\beta) \right]. \quad (6)$$

Here, the vortex system is considered from a reference frame that moves with the background flow (i.e.,  $W_\infty = 0$ ). Since the vortex strengths are assumed to be invariant, the sum of vortex strengths  $\Gamma_\infty$  is a constant of motion that, in an effort to model the periodic shedding of vorticity into the wake, is taken to be zero:

$$\Gamma_\infty = \sum_{\alpha=1}^N \Gamma_\alpha = 0. \quad (7)$$

We note that (6) can be expressed in Hamiltonian form,

$$\Gamma_\alpha \frac{dx_\alpha}{dt} = \frac{\partial \mathcal{H}}{\partial y_\alpha}, \quad \Gamma_\alpha \frac{dy_\alpha}{dt} = -\frac{\partial \mathcal{H}}{\partial x_\alpha}. \quad (8)$$

with the Hamiltonian for the singly-periodic vortex system—a constant of motion—given as,

$$\mathcal{H}(z_1, \dots, z_N; \Gamma_1, \dots, \Gamma_N) = -\frac{1}{4\pi} \sum_{\alpha=1}^N \sum_{\substack{\beta=1 \\ \beta \neq \alpha}}^N \Gamma_\alpha \Gamma_\beta \ln \left| \sin \left[ \frac{\pi}{L} (z_\alpha - z_\beta) \right] \right|. \quad (9)$$

Hence, given a set of vortex strengths  $\Gamma_\alpha$ , the topology of phase-space becomes fixed. Then, a particular trajectory in phase-space is dictated by the initial positions of the point vortices  $z_\alpha$ . Stated another way, the vortex strengths determine which classes of motion are possible, while the initial vortex positions determine which particular class of motion among these is realized. At this point, it should be apparent that the WR scheme does not encapsulate enough information to describe the wake dynamics; rather, in order to characterize the dynamic evolution of the wake, information related to the relative strengths and positions of the  $N$  point vortices shed per cycle is also needed.

Idealized point vortex models have been developed to study the dynamics of various wakes, including 2S, 2P, and P+S. Here, we follow the works by Stremler and colleagues<sup>28–30</sup> to model a 2P wake, with the aim of using this model to validate the wake regime learning framework presented in Section II.

The dynamics of 2P wakes ( $N = 4$ ) can be reduced to an integrable two-degree-of-freedom Hamiltonian system by taking the base vortex positions and strengths to be

$$\Gamma_3 = -\Gamma_1, \quad \Gamma_4 = -\Gamma_2 \quad (10)$$

$$z_3 = z_1^* - \frac{L}{2}, \quad z_4 = z_2^* + \frac{L}{2}. \quad (11)$$

Defining  $S := \Gamma_1 + \Gamma_2$ , it follows that the non-dimensional linear impulse for the base vortices  $\mathcal{Q} + i\mathcal{P} = (\pi/LS) \sum_{\alpha=1}^N \Gamma_\alpha z_\alpha$  reduces to

$$\mathcal{Q} = \frac{\pi}{2} (2\gamma - 1) \quad (12)$$

$$\mathcal{P} = \frac{2\pi}{L} [\gamma y_1 + (1 - \gamma)y_2], \quad (13)$$

where  $\gamma := \Gamma_1/S$ . For convenience, we take  $0 \leq \Gamma_1 \leq \Gamma_2$ , such that  $0 \leq \gamma \leq 1/2$ . Then, upon defining  $Z := X + iY = \pi(z_1 - z_2)/L$  as the normalized separation between the first and second based-vortices, the Hamiltonian takes the form<sup>30</sup>

$$\mathcal{H} = \mathcal{H}(X, Y; \gamma, \mathcal{P}). \quad (14)$$

In other words, for the idealized 2P wake model, the evolution of the associated system of point vortices can be reduced to tracking the separations between the base pairs of vortices. Further, the motion is parameterized by the linear impulse of the base pairs, though it is more convenient to express this parameterization in terms  $\gamma$  and  $\mathcal{P}$ . While  $\gamma$  and  $\mathcal{P}$  determine the types of dynamical regimes that can be exhibited, the particular regime of motion is dictated by the value of the Hamiltonian, which is a constant of the motion.

In Section IV, the idealized 2P wake model will be used to explore and test the snapshot-based wake regime learning framework. We appeal to feature vectors based on low-rank POD representations of the data, as in (1); no prior knowledge of the wake dynamics nor the underlying evolution equations is assumed.

## IV. Results: Utilizing Snapshot Data to Learn Idealized 2P Wake Regimes

The idealized 2P wake model summarized at the end of Section III displays a rich set of dynamical regimes, providing an ideal model system for wake regime learning algorithm development and validation. Our focus on 2P wakes is further motivated by the fact that such wakes are among the most commonly encountered exotic wake patterns in a number of contexts, including swimming locomotion and vortex induced vibrations.<sup>16</sup>

Recently, Basu and Stremler performed an extensive characterization of the dynamics associated with the idealized 2P wake model, reporting twelve distinct regimes of motion, which can be reduced to five general classes of motion, named according to patterns displayed in the vortex trajectories: Orbiting ( $O_1, O_2, O_3, O_4$ ), Exchanging ( $E_1, E_2, E_3, E_4$ ), Mixed ( $M_1, M_2$ ), Passing ( $P_1, P_2$ ), and Scattering ( $S_1, S_2$ ). The scattering and passing patterns arise in limiting cases with  $\gamma = 0$  and  $\gamma = 1/2$ ; they will not be considered further in the present study. Further, the mixed regimes  $M_1$  and  $M_2$  were aptly named owing to a “mix” of orbiting and exchanging trajectories: in a single period, the mixed trajectory follows an orbiting pattern for a portion of the motion, then switches to an exchanging pattern. Owing to this complicated behavior, we defer the mixed regime to future study, and instead focus attention to the orbiting and exchanging regimes of motion.

### A. Three Orbiting Sub-Regimes: $O_1, O_2$ , and $O_3$

The first case to be considered consists of 15 wake realizations, five from each of three different orbiting wake regimes ( $O_1, O_2, O_3$ ). The Hamiltonian level curves in phase-space and representative vortex trajectories in physical space are presented in Figure 2. The vortex trajectories for each of these 2P wakes clearly demonstrates the differences in the evolution patterns of these different wake regimes: even among orbiting 2P wakes, the vortex trajectories are notably distinct. A representative sub-sampled velocity snapshot sequence from each sub-regime  $O_1, O_2$ , and  $O_3$  is shown in Figure 3. While a close comparison of the snapshot *sequences* reveals differences in the wake evolution patterns, a comparison of a single snapshot from each sequence can lead to different conclusions. For instance, the first snapshot in  $O_1, O_2$ , and  $O_3$  are quite similar, and compared alone may lead to the false conclusion that these are equivalent wakes. This observation confirms the need for a *sequence* of snapshots in the wake regime learning task. The corresponding feature vector from each of these snapshot sequences is also presented in Figure 3, demonstrating that the sequence can be reduced to a single spatial mode that can potentially be used to distinguish between the wake regimes. For the particular samples presented in Figure 3, the feature vectors (i.e., the absolute value of the dominant POD mode) are qualitatively distinct from one another.

The resulting wake clusters, with the assumed number of clusters  $K = \{2, 3, 4\}$ , are reported in Figure 4. For all  $K$ , the  $O_1$  and  $O_2$  regimes are fully distinguishable from each other; however, the resulting clusters conflate certain realizations of the  $O_3$  regime with the  $O_1$  and  $O_2$  regimes. It is interesting to note that the first two and the last three realizations from  $O_2$  and  $O_3$ , respectively, correspond to the realizations residing closest to the regime boundaries, as seen in the Hamiltonian level sets in Figure 2. While promising, these results suggest that the absolute value of the dominant POD mode alone is insufficient to fully distinguish between orbiting wake sub-regimes. We note that including additional POD modes does not alter these results. Further, the results based on the dominant POD mode yielded superior performance over alternative feature choices, such as Fourier modes/frequencies or DMD modes/eigenvalues.

### B. An Exchanging Regime and Three Orbiting Sub-Regimes: $E_1, O_1, O_2$ , and $O_4$

In the previous section, we considered the problem of distinguishing between orbiting sub-regimes. Of course, distinguishing between sub-regimes of a particular class of motion may be more challenging than distinguishing between two broader classes of motion. Here, we consider the wake regime learning problem in the context of data associated with an exchanging wake ( $E_1$ ) and three orbiting sub-regimes ( $O_1, O_2, O_4$ ). The level curves of the Hamiltonian in phase-space are presented in Figure 5, along with representative vortex trajectories in physical space. The patterns exhibited by the vortex trajectories highlight a clear difference between the exchanging  $E_1$  wake and each of the orbiting sub-regimes. The patterns also indicate that the  $O_1$  and  $O_4$  patterns may be challenging to distinguish from one another, but that  $O_2$  will likely be straightforward to isolate.

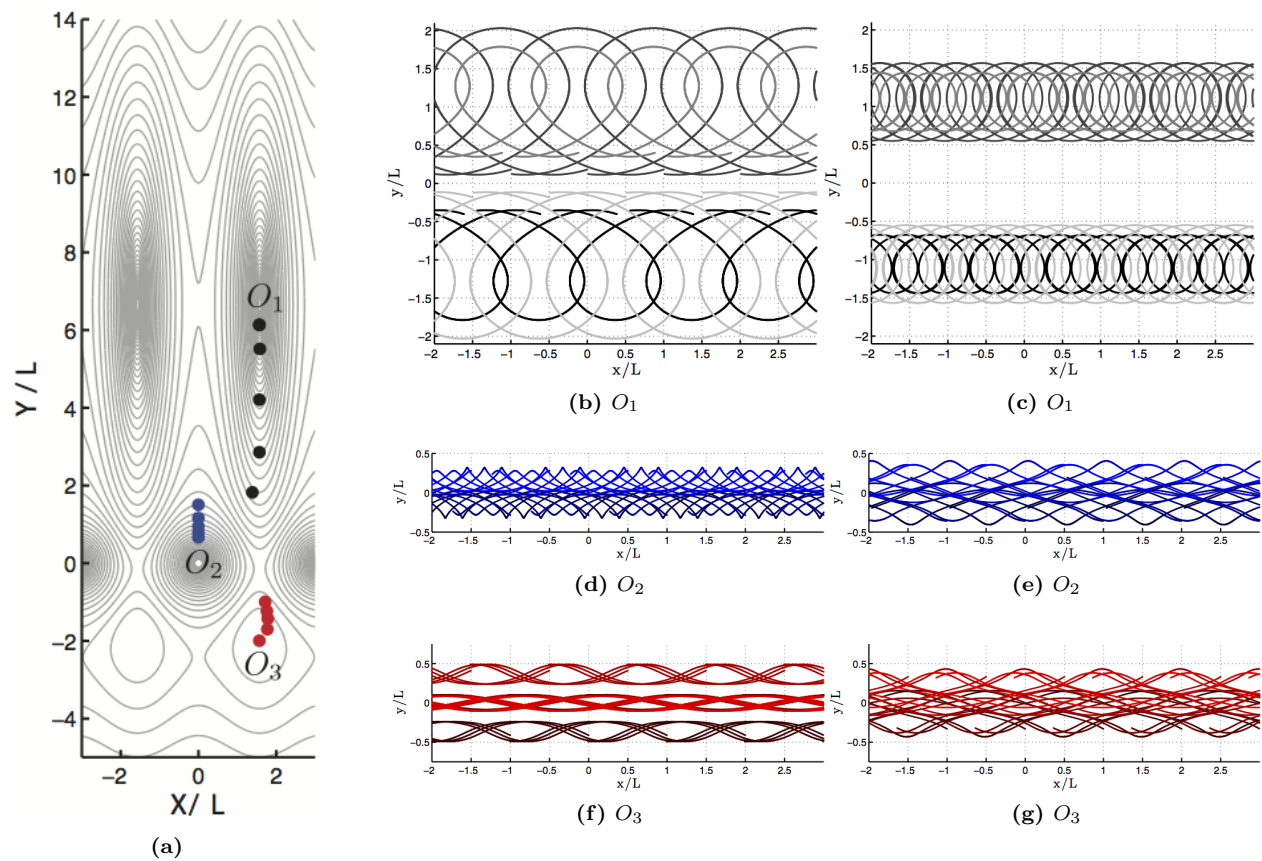


**Figure 2:** The idealized 2P wake model is used to generate three different orbiting regimes ( $O_1$ ,  $O_2$ ,  $O_3$ ) by setting  $\mathcal{H}(X, Y; 3/7, -0.95)$ . In (a), Hamiltonian level curves are plotted in phase-space; circles denote the initial phase-space coordinate for each realization that is considered. In (b)–(g), representative vortex trajectories for each of the orbiting sub-regimes are shown. For the most part, the trajectories display different patterns, though similarities are observed as well—compare (e) and (g), for instance.

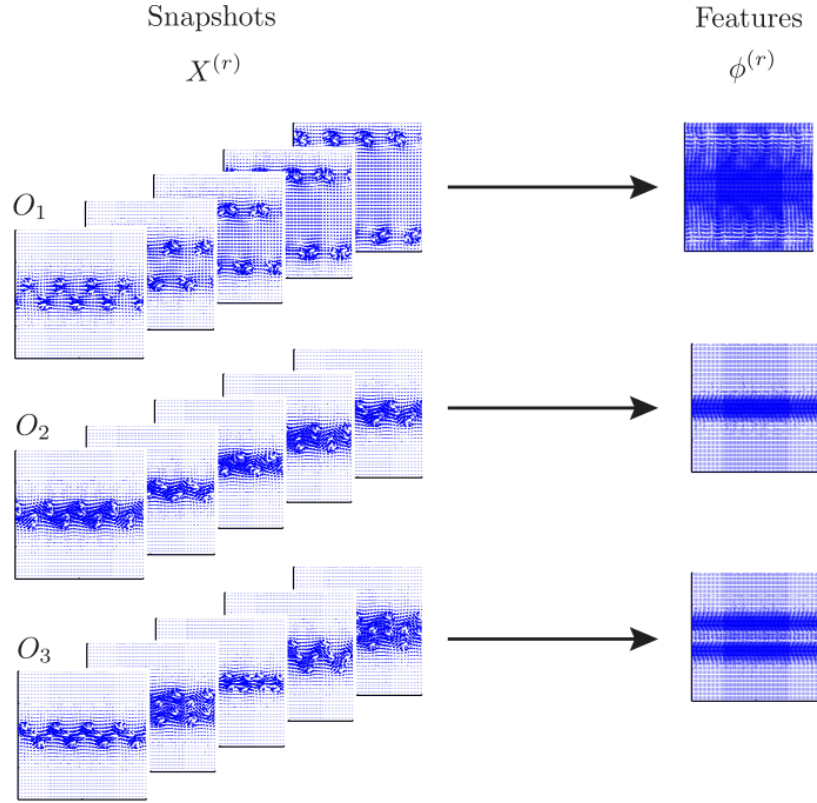


**Figure 3:** A sample of velocity snapshot realizations from each orbiting wake regime ( $O_1$ ,  $O_2$ ,  $O_3$ ) and associated feature vectors computed according to (1).

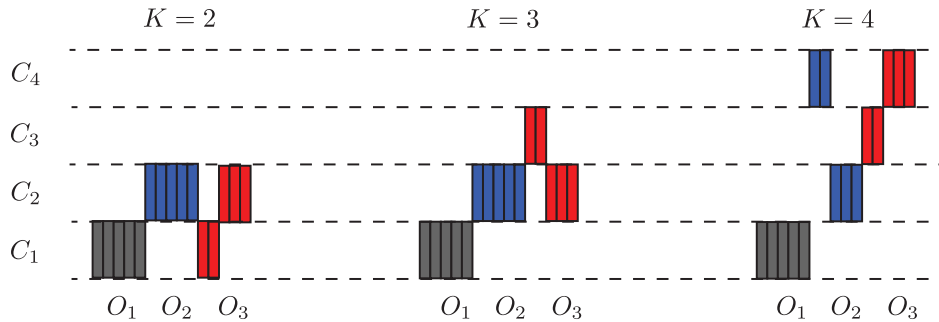


**Figure 4:** Orbiting wake regime learning results for different numbers of clusters  $K = \{2, 3, 4\}$ .  $O_1$  is always correctly distinguished from both  $O_2$  and  $O_3$ . On the other hand, many  $O_2$  and  $O_3$  realizations are grouped together; interestingly, these same realizations are evolve close to the regime boundaries (see Figure 2).

A set of sub-sampled snapshot sequences from each of these regimes is presented in Figure 6. Here too, visual inspection suggests the  $E_1$  and  $O_2$  regimes are most distinct, while  $O_1$  and  $O_4$  are most similar. The feature vectors in Figure 6 seem to indicate a similar conclusion. Closer inspection of the Hamiltonian level curves associated with  $O_1$  and  $O_4$  (see Figure 5) reveals an explanation for this similarity: the  $O_1$  and  $O_4$  phase-space orbits essentially follow the same trajectories in phase-space, except that  $O_4$  takes a small excursion into the lower portion of phase-space.

The wake regime learning results for this set of wake data are presented in Figure 7, for  $K = \{2, 3, 4\}$ . As anticipated based on visual comparisons of trajectories, snapshot sequences, and feature vectors, the exchanging regime ( $E_1$ ) is always distinguished from the orbiting sub-regimes ( $O_1, O_2, O_3$ ). Further, when  $K = 3$ , the  $O_1$  and  $O_4$  regimes are consistently most similar to one another, and are clustered accordingly; the  $E_1$  and  $O_2$  regimes are correctly distinguished as such as well. Finally, when  $K = 4$ , all of the regimes are correctly clustered, except for a single realization of  $O_1$  and a single realization of  $O_4$ ; the particular  $O_1$  and  $O_4$  realizations that are incorrectly clustered correspond to the realizations closest to the regime boundaries. Given the similarity in trajectories between  $O_1$  and  $O_4$ , the success of the wake regime learning method here is noteworthy.

## V. Concluding Discussion

The results presented in Section IV demonstrate that the wake regime learning framework can be designed to sort wake snapshot data according to dynamical similarities. In particular, snapshot data from orbiting and exchanging regimes can be distinguished from one another. Moreover, except in the challenging scenario that a wake realization evolves close to a regime boundary, snapshots realizations from orbiting sub-regimes can be distinguished from one another as well. To improve performance, further investigation is needed from the standpoint of feature extraction and clustering. Here, we only reported results based on simple features extracted from snapshot sequences (i.e., absolute value of the dominant POD mode), subsequently processed using the  $k$ -means clustering technique. Another important consideration to be addressed in the future is a strategy to reliably determine and select the number of clusters (i.e., dynamical regimes) present in the dataset under consideration; such considerations are necessary for making the wake regime learning framework purely data-driven and fully objective.

While further investigation is needed to reconcile the issues and challenges described above, the results presented in Section IV—based on simple features and clustering techniques—suggest that the perspective of wake regime learning may facilitate the development of a new dynamics-based wake labeling convention in the future. A reliable wake regime learning technique will aid studies of swimming locomotion by allowing objective dynamical comparisons of wakes, even across contexts and application domains. At the very least, a reliable wake regime learning algorithm can be invoked to construct a library of wake labels for use in various wake classification tasks.

Additionally, the perspective taken here has been based entirely on the snapshot data itself, without any prior knowledge or regard for the nature of the underlying dynamics. As such, at least in principle, the wake regime learning framework presented here—consisting of a feature extraction stage and a clustering stage—can be extended to the general problem of *flow regime learning*. Of course, additional investigation is needed to establish the validity and viability of doing so.

Lastly, while we have introduced the wake regime learning framework as a means for objectively exploring and comparing empirical wake data, we have not gone so far as to introduce a dynamically relevant labeling convention that is as simple to employ as identifying the number and grouping of vortices shed per cycle. Whether or not it will be possible to develop a *simple* dynamics-based labeling criterion is yet to be determined; however, we are hopeful that the perspective presented here will help uncover new insights from empirical wake data that will move us in that direction.

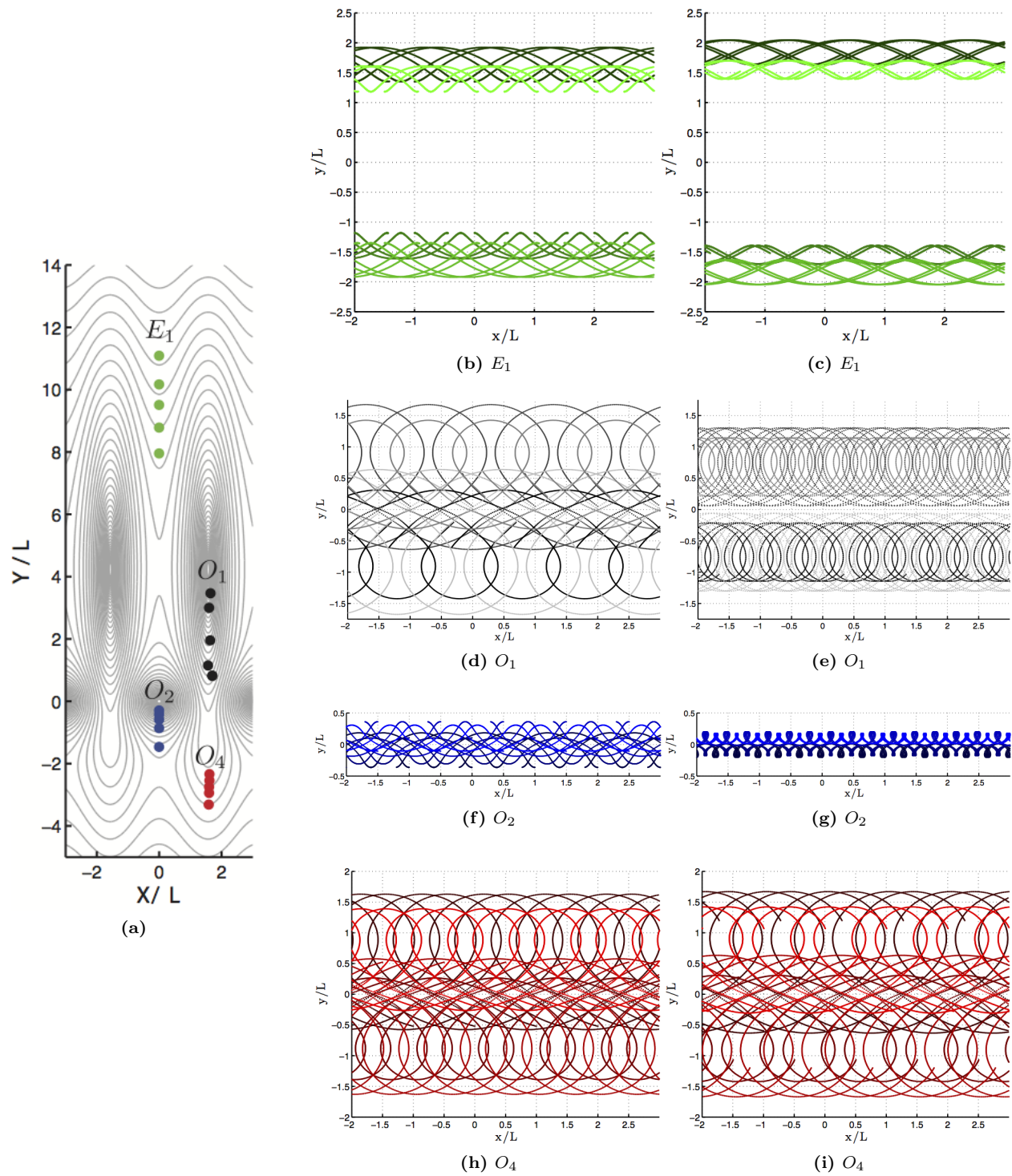


**Figure 5:** The idealized 2P wake model is used to generate an exchanging regime ( $E_1$ ) and three different orbiting regimes ( $O_1$ ,  $O_2$ ,  $O_4$ ) by setting  $\mathcal{H}(X, Y; 3/7, -0.605)$ . In (a), Hamiltonian level curves are plotted in phase-space; circles denote the initial phase-space coordinate for each realization that is considered. In (b)–(i), representative vortex trajectories for each of the exchanging and orbiting sub-regimes are shown. For the most part, the trajectories display different patterns, though similarities are observed as well—compare (d) with (h) and (i), for instance.

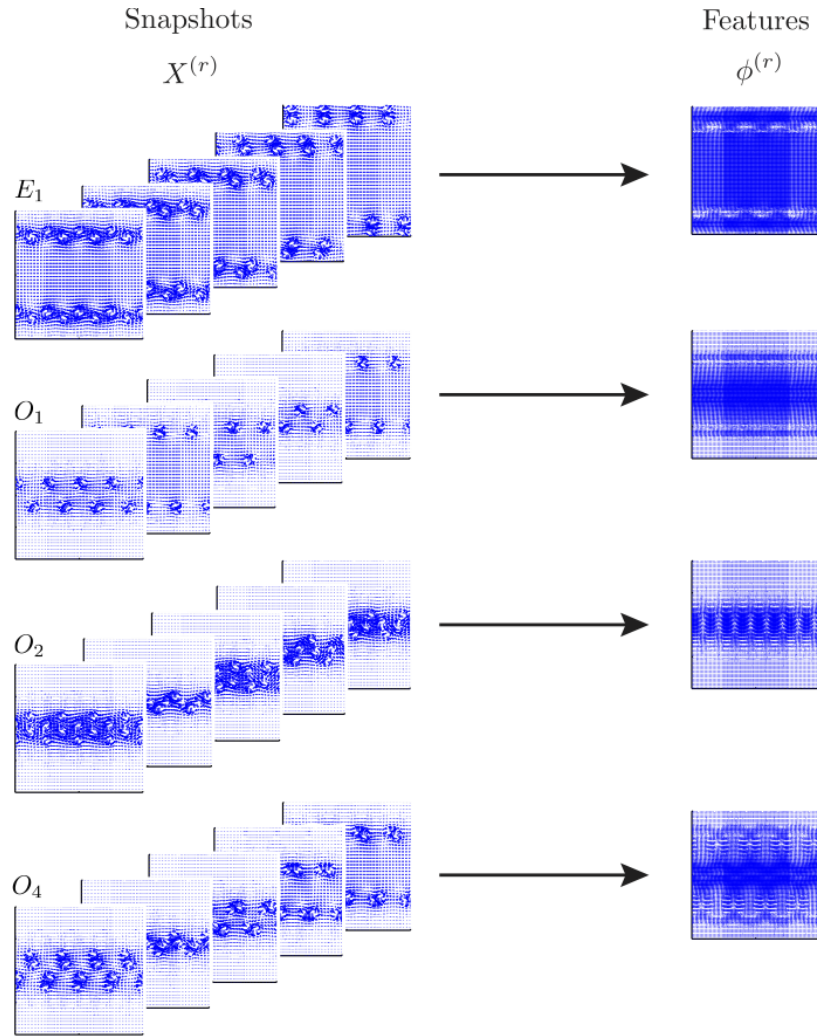


**Figure 6:** A sample of snapshot realizations from each of the exchanging and orbiting wake regimes and associated feature vectors computed according to (1).

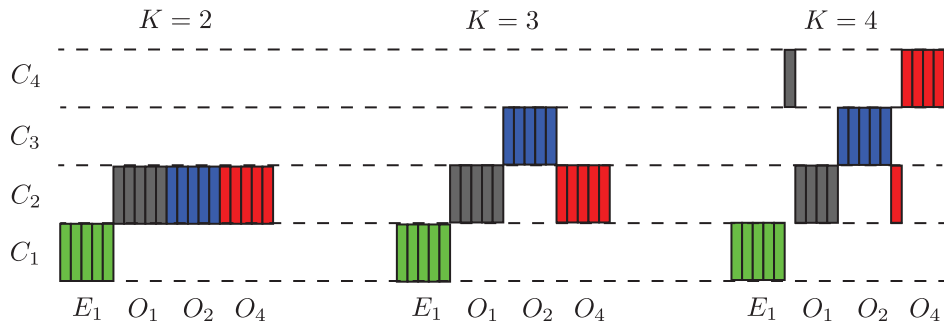


**Figure 7:** Exchanging and orbiting wake regime learning results for different numbers of clusters  $K = \{2, 3, 4\}$ . The exchanging  $E_1$  regime is always correctly distinguished from all of the orbiting sub-regimes. The  $O_2$  sub-regime is correctly grouped with the other orbiting sub-regimes when  $K = 2$ , and is identified as distinct from  $O_1$  and  $O_4$  in all other instants. The  $O_1$  and  $O_4$  sub-regimes are grouped together when  $K = \{2, 3\}$  and are almost fully distinguished when  $K = 4$ . The  $O_1$  and  $O_4$  realizations that are falsely clustered when  $K = 4$  evolve close to the regime boundaries (see Figure 5).

## References

- <sup>1</sup>Breder, C. M., “The Locomotion of fishes,” *Zoologica*, Vol. 4, 1926, pp. 159–256.
- <sup>2</sup>Blake, R. W., *Fish Locomotion*, Cambridge University Press, New York, 1983.
- <sup>3</sup>Müller, U., van den Heuvel, B., Stamhuis, E., and Videler, J., “Fish foot prints: morphology and energetics of the wake behind a continuously swimming mullet,” *Journal of Experimental Biology*, Vol. 200, 1997, pp. 2893–2906.
- <sup>4</sup>Drucker, E. and Lauder, G., “Locomotor forces on a swimming fish: three-dimensional vortex wake dynamics quantified using digital particle image velocimetry,” *The Journal of experimental biology*, Vol. 202, No. Pt 18, 1999, pp. 2393–2412.
- <sup>5</sup>Drucker, E. G. and Lauder, G. V., “Wake dynamics and fluid forces of turning maneuvers in sunfish,” *The Journal of experimental biology*, Vol. 204, No. Pt 3, 2001, pp. 431–442.
- <sup>6</sup>Müller, U. K., Smit, J., Stamhuis, E. J., and Videler, J. J., “How the body contributes to the wake in undulatory fish swimming: flow fields of a swimming eel (*Anguilla anguilla*),” *Journal of Experimental Biology*, Vol. 204, No. Pt 16, 2001, pp. 2751–2762.
- <sup>7</sup>Drucker, E. G. and Lauder, G. V., “Experimental hydrodynamics of fish locomotion: functional insights from wake visualization,” *Integrative and comparative biology*, Vol. 42, No. 2, 2002, pp. 243–257.
- <sup>8</sup>Hultmark, M., Leftwich, M. C., and Smits, A. J., “Flowfield measurements in the wake of a robotic lamprey,” *Experiments in Fluids*, Vol. 43, No. 5, 2007, pp. 683–690.
- <sup>9</sup>Müller, U. K., van den Boogaart, J. G. M., and van Leeuwen, J. L., “Flow patterns of larval fish: undulatory swimming in the intermediate flow regime,” *Journal of Experimental Biology*, Vol. 211, No. Pt 2, 2008, pp. 196–205.
- <sup>10</sup>Tytell, E. D., Borazjani, I., Sotiropoulos, F., Baker, T. V., Anderson, E. J., and Lauder, G. V., “Disentangling the Functional Roles of Morphology and Motion in the Swimming of Fish,” *Integrative and Comparative Biology*, Vol. 50, No. 6, 2010, pp. 1140–1154.
- <sup>11</sup>Leftwich, M. C., Tytell, E. D., Cohen, A. H., and Smits, A. J., “Wake structures behind a swimming robotic lamprey with a passively flexible tail,” *Journal of Experimental Biology*, Vol. 215, No. 3, 2012, pp. 416–425.
- <sup>12</sup>van Rees, W. M., Gazzola, M., and Koumoutsakos, P., “Optimal shapes for anguilliform swimmers at intermediate Reynolds numbers,” *Journal of Fluid Mechanics*, Vol. 722, No. May, 2013, pp. R3.
- <sup>13</sup>Bearman, P. W., “Vortex shedding from oscillating bluff bodies,” *Annual Review of Fluid Mechanics*, Vol. 16, 1984, pp. 195–222.
- <sup>14</sup>Williamson, C. H. K., “Sinusoidal flow relative to circular cylinders,” *Journal of Fluid Mechanics*, Vol. 155, 1985, pp. 141–174.
- <sup>15</sup>Koochesfahani, M. M., “Vortical patterns in the wake of an oscillating airfoil,” *AIAA Journal*, Vol. 27, No. 9, 1989, pp. 1200–1205.
- <sup>16</sup>Williamson, C. and Govardhan, R., “Vortex-Induced Vibrations,” *Annual Review of Fluid Mechanics*, Vol. 36, No. 1, 2004, pp. 413–455.
- <sup>17</sup>Spedding, G. R., “Wake Signature Detection,” *Annual Review of Fluid Mechanics*, Vol. 46, 2014, pp. 273–302.
- <sup>18</sup>Williamson, C. H. K. and Roshko, A., “Vortex formation in the wake of an oscillating cylinder,” *Journal of Fluids and Structures*, Vol. 2, 1988, pp. 355–381.
- <sup>19</sup>Lentink, D., Muijres, F. T., Donker-Duyvis, F. J., and van Leeuwen, J. L., “Vortex-wake interactions of a flapping foil that models animal swimming and flight,” *Journal of Experimental Biology*, Vol. 211, No. Pt 2, 2008, pp. 267–273.
- <sup>20</sup>Schnipper, T., Andersen, A., and Bohr, T., “Vortex wakes of a flapping foil,” *Journal of Fluid Mechanics*, Vol. 633, 2009, pp. 411–423.
- <sup>21</sup>Moored, K. W., Dewey, P. A., Smits, A. J., and Haj-Hariri, H., “Hydrodynamic Wake Resonance as an Underlying Principle of Efficient Unsteady Propulsion,” *Journal of Fluid Mechanics*, Vol. 708, 2012, pp. 329–348.
- <sup>22</sup>Smits, A. J., Moored, K. W., and Dewey, P. A., *Fluid-Structure-Sound Interactions and Control: Proceedings of the 2nd Symposium on Fluid-Structure-Sound Interactions and Control*, chap. The Swimming of Manta Rays, Springer Berlin Heidelberg, Berlin, Heidelberg, 2014, pp. 291–300.
- <sup>23</sup>Valdivia y Alvarado, P. and Youcef-Toumi, K., “Soft-Body Robot Fish,” *Robot Fish: Bio-inspired Fishlike Underwater Robots*, edited by R. Du, Z. Li, K. Youcef-Toumi, and P. Valdivia y Alvarado, Springer Berlin Heidelberg, Berlin, Heidelberg, 2015, pp. 161–191.
- <sup>24</sup>Ren, Z., Yang, X., Wang, T., and Wen, L., “Hydrodynamics of a robotic fish tail: effects of the caudal peduncle, fin ray motions and the flow speed,” *Bioinspiration & Biomimetics*, Vol. 11, No. 1, 2016, pp. 016008.
- <sup>25</sup>Aref, H., “Integrable, chaotic, and turbulent vortex motion in two-dimensional flows,” *Annual Review of Fluid Mechanics*, Vol. 15, No. 1, 1983, pp. 345–389.
- <sup>26</sup>Aref, H. and Stremler, M. A., “Four-vortex motion with zero total circulation and impulse,” *Physics of Fluids*, Vol. 11, No. 12, 1999, pp. 3704.
- <sup>27</sup>Aref, H., Stremler, M. A., and Ponta, F. L., “Exotic vortex wakes—point vortex solutions,” *Journal of Fluids and Structures*, Vol. 22, No. 6-7, 2006, pp. 929–940.
- <sup>28</sup>Stremler, M. A., Salmanzadeh, A., Basu, S., and Williamson, C. H. K., “A mathematical model of 2P and 2C vortex wakes,” *Journal of Fluids and Structures*, Vol. 27, No. 5-6, 2011, pp. 774–783.
- <sup>29</sup>Stremler, M. A. and Basu, S., “On point vortex models of exotic bluff body wakes,” *Fluid Dynamics Research*, Vol. 46, No. 6, 2014, pp. 061410.
- <sup>30</sup>Basu, S. and Stremler, M. A., “On the motion of two point vortex pairs with glide-reflective symmetry in a periodic strip On the motion of two point vortex pairs with glide-reflective symmetry in a periodic strip,” *Physics of Fluids*, , No. 103603, 2015.
- <sup>31</sup>Huera-Huarte, F. J. and Vernet, A., “Vortex modes in the wake of an oscillating long flexible cylinder combining POD and fuzzy clustering,” *Experiments in Fluids*, Vol. 48, No. 6, 2010, pp. 999–1013.

- <sup>32</sup>Tauro, F., Grimaldi, S., and Porfiri, M., “Unraveling flow patterns through nonlinear manifold learning,” *PLoS ONE*, Vol. 9, No. 3, 2014, pp. 1–6.
- <sup>33</sup>Bright, I., Lin, G., and Kutz, J. N., “Compressive Sensing and Machine Learning Strategies for Characterizing the Flow around a Cylinder with Limited Pressure Measurements,” *Physics of Fluids*, Vol. 25, 2013.
- <sup>34</sup>Bright, I., Lin, G., and Kutz, J. N., “Classification of Spatio-Temporal Data via Asynchronous Sparse Sampling,” *pre-print, arXiv: 1506.00661*, 2015.
- <sup>35</sup>Bai, Z., Brunton, S. L., Brunton, B. W., Kutz, J. N., Kaiser, E., Spohn, A., and Noack, B. R., “Data-Driven Methods in Fluid Dynamics: Sparse Classification from Experimental Data,” *Whither Turbulence and Big Data in the 21st Century*, 2015.
- <sup>36</sup>Markovsky, I., *Low Rank Approximation: Algorithms, Implementation, Applications*, Springer, 2012.
- <sup>37</sup>Schmid, P., “Dynamic mode decomposition of numerical and experimental data,” *Journal of Fluid Mechanics*, Vol. 656, 2010, pp. 5–28.
- <sup>38</sup>Tu, J. H., Rowley, C. W., Luchtenburg, D. M., Brunton, S. L., and Kutz, J. N., “On dynamic mode decomposition: theory and applications,” *Journal of Computational Dynamics*, Vol. 1, No. 2, 2014, pp. 391–421.
- <sup>39</sup>Bishop, C. M., *Pattern Recognition and Machine Learning*, Springer, 2006.
- <sup>40</sup>Tan, P.-N., Steinbach, M., and Kumar, V., *Introduction to Data Mining*, Pearson, Boston, 2006.
- <sup>41</sup>Newton, P. K., *The N-Vortex Problem: Analytical Techniques*, Springer-Verlag, New York, 2001.
- <sup>42</sup>Cottet, G.-H. and Koumoutsakos, P. D., *Vortex Methods: Theory and Practice*, Cambridge University Press, New York, 2000.